The University of Akron
IdeaExchange@UAkron

Chemical and Biomolecular Engineering Faculty Research

Chemical and Biomolecular Engineering Department

1-15-2008

Electrical, Structural, and Chemical Properties of Semiconducting Metal Oxide Nanofiber Yarns

A. F. Lotus

E. T. Bender

E. A. Evans

R. D. Ramsier

D. H. Reneker

See next page for additional authors

Please take a moment to share how this work helps you through this survey. Your feedback will be important as we plan further development of our repository.

Follow this and additional works at: http://ideaexchange.uakron.edu/chemengin_ideas

Part of the Chemistry Commons

Recommended Citation

Authors

A. F. Lotus, E. T. Bender, E. A. Evans, R. D. Ramsier, D. H. Reneker, and George G. Chase

Electrical, structural, and chemical properties of semiconducting metal oxide nanofiber yarns

A. F. Lotus,[1] E. T. Bender,[2] E. A. Evans,[1] R. D. Ramsier,[2] D. H. Reneker,[3] and G. G. Chase[1,a)]

[1]*Department of Chemical and Biomolecular Engineering, The University of Akron, Akron, Ohio 44325-3906, USA*
[2]*Department of Physics, The University of Akron, Ohio 44325-4001, USA*
[3]*Department of Polymer Science, The University of Akron, Akron, Ohio 44325-3909, USA*

The electrical, structural, and chemical properties of twisted yarns of metal-oxide nanofibers, fabricated using a modified electrospinning technique, are investigated in this report. In particular, synthesized zinc oxide and nickel oxide yarns having diameters in the range of $4-40$ μm and lengths up to 10 cm were characterized, whose constituent nanofibers had average diameters of $60-100$ nm. These yarns have one macroscopic dimension for handling while retaining some of the properties of nanofibers. © *2008 American Institute of Physics*. [DOI: 10.1063/1.2831362]

I. INTRODUCTION

The electrospinning method has attracted much attention in the past several years for generating micro- and nanofibers of organic polymers, composites, and inorganic oxide materials.[1–4] The basic principle behind electrospinning is relatively simple and consists of three major components: A high-voltage power supply, a hollow needle or conical holder for the precursor solution, and a grounded conductor that serves as a collector. When a sufficiently high voltage (on the order of 20 kV) is applied to the precursor solution, the electrostatic force within the polymer solution overcomes the surface tension of the solution, causing the ejection of a thin liquid jet from the tip of the needle. The charged jet then undergoes a stretching process affected by several parameters which include interactions with the external electric field, electrostatic forces within the polymer solution, solution viscosity, and surface tension of the solution.[5] The liquid jet is continuously elongated and thus becomes thinner until most of the solvent is evaporated and fibers are formed. Generally the resulting fibers collect on the grounded collector as a planar web of micro- or nanofibers in random orientations. This random orientation is acceptable for certain applications such as composite reinforcement, catalyst support, filtration, and biomedical applications (e.g., tissue engineering scaffolds, wound dressings, drug delivery materials). For other applications, such as electronic, optoelectronic, photonic, sensors, etc., it is more desirable to obtain nanofiber samples in which the fiber axes are aligned in the same direction which is referred to as "axial orientation."[6]

It is possible to obtain ordered structures by making yarns from a bundle of axially oriented electrospun nanofibers. A fiber bundle or yarn can be more easily handled as it has greater mechanical strength than single nanofibers or nanofiber mats.[7] A few investigations on the fabrication of twisted yarns of polymer nanofibers are reported. Twisted yarns of unidirectional and molecularly oriented polyacrylonitrile nanofibers were made using a high speed (0–2284 rpm), rotating take-up wheel.[8] The fiber bundles were then collected from the wheel, linked together, and twisted using an electric spinner to obtain a twisted yarn. Electrospinning between dual collection rings to form three dimensional unidirectional arrays of polycaprolactone microfibers is also reported.[9] Rotation of one of the collection rings resulted in a wound multifilament yarn with a diameter below 5 μm and a length of 50 mm.

Our electrospinning arrangement for making twisted yarns is shown in Fig. 1 and is described in detail in the experimental section. It includes two collector surfaces; one of which is a rotating hollow hemisphere, while the other is a nonrotating but translating metal rod. The rod is translated in the direction of its axis away from the hollow hemisphere to extend the length of the developing yarn.[10] Yarns of nanofibers can be obtained from many polymers and polymeric precursors of metal oxides. In this paper we report on
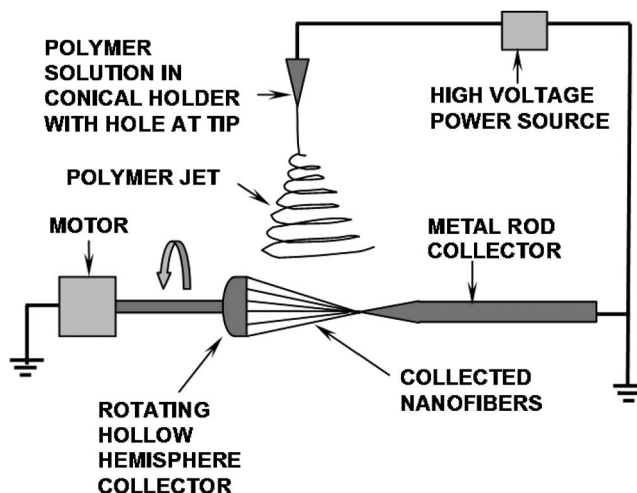

FIG. 1. Schematic diagram of the apparatus for producing nanofiber yarns.

a)Author to whom correspondence should be addressed. Tel.: 330-972-7943. FAX: 330-972-5856. Electronic mail: gchase@uakron.edu.
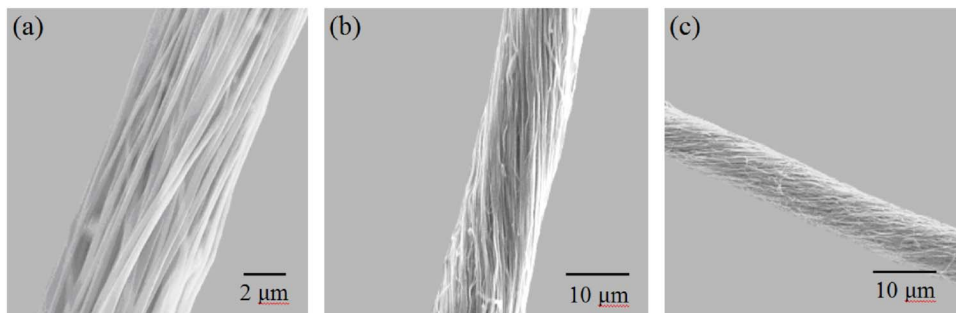
FIG. 2. (Color online) (a) A yarn of electrospun fibers made from a homogeneous mixture of zinc acetate and PVP solution (before heat treatment), (b) zinc oxide nanofiber yarn annealed at 873 K, and (c) nickel oxide nanofiber yarn annealed at 873 K.

the fabrication, physical, chemical, and electrical property characterization of semiconducting metal oxide (zinc oxide, nickel oxide) nanofiber yarns.

II. EXPERIMENTAL

A. Electrospinning apparatus

To make the yarns, electrospinning was performed between two collector surfaces placed about 8 cm apart horizontally opposite to one another, as shown in Fig. 1. One collector was a metal rod of 3 mm in diameter and 20 cm in length and was supported on an insulated surface. The end of the rod was tapered over a length of 1 cm to a sharp point and was not insulated, while the shaft of the rod was covered with insulating tape. The second collector was a 5 cm diameter hollow metal hemisphere attached to the end of a 10 mm diameter, 20 cm long hollow metal tube. The outer surfaces of the metal tube and all but a 2 mm band at the hemisphere's edge were covered with insulating tape. The purpose of the insulation was to increase the probability that the electrospinning jet would deposit at the edge of the hemisphere and on the tapered tip of the rod.

The electrospinning was accomplished by filling a metal conical shaped holder having a 1 mm hole at the tip with the polymer solution and positioning the holder vertically above the two grounded collector surfaces at a distance of about 25 cm. A positive voltage of 10–15 kV was applied to the conical holder. Electrospun fibers were collected between the two collector surfaces. The hollow metal hemisphere was rotated at 100–1000 rpm to twist the fibers together. The twisted yarn was suspended between the hemisphere and the tapered rod. The tapered rod was moved away from the rotating collector at a rate of 5 mm/s, while the fibers continued to collect, and a continuous length of yarn was produced.

B. Synthesis

To make the metal oxide fibers, zinc or nickel acetate (Aldrich) was mixed into polymer solutions of polyvinylpyrrolidone (PVP) (Aldrich, molecular weight: 1×10^6). The composite polymer nanofiber yarns were annealed at 873 K for 2 h (which is above the degradation temperature of the PVP—verified by thermogravimetric analysis) at a heating rate of 5 K/min, resulting in the formation of the metal oxide nanofiber yarns.

III. RESULTS AND DISCUSSION

A. Structural property characterization

1. Scanning electron microscopy

For scanning electron microscopy (SEM) (Hitachi S-2150) analysis, the nanofibers and yarns were placed on an aluminum stub with a strip of carbon tape applied to the surface to promote fiber adhesion while minimizing charging effects. The samples were silver coated (S150B Sputter Coater, Edwards) and imaged using an accelerating voltage of 20 kV. Average diameters were calculated from 50 data points.

Figure 2 shows representative SEM images of the nanofiber yarns. The zinc oxide nanofibers had an average diameter of 63.2 nm and standard deviation of 6.6 nm, whereas the nickel oxide nanofibers had an average diameter of 98.6 nm and standard deviation of 4.6 nm. The average diameters of the corresponding yarns were dependent on the duration of electrospinning. Zinc oxide nanofiber yarns had a average bulk density of 0.43 g/cm^3 and that of nickel oxide was 0.34 g/cm^3.

Holding other parameters constant (e.g., solution composition, viscosity, voltage, distance from the liquid jet to the grounded collectors, distance between two collector surfaces, and the rotational speed of collector), the resulting yarn diameters are plotted in Fig. 3. The yarn diameters increase with electrospinning time as expected; however, for a con-
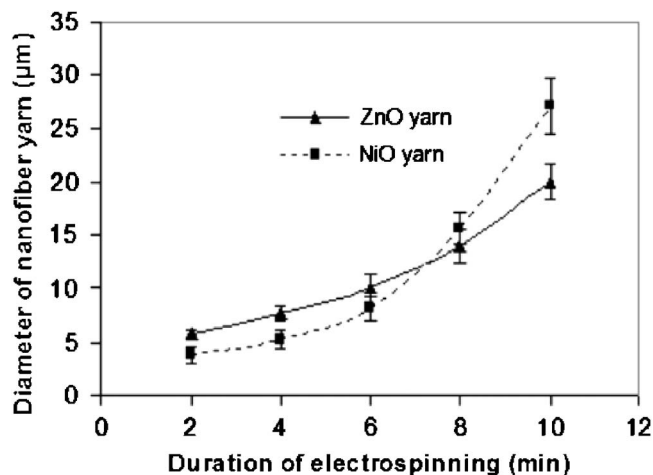

FIG. 3. Average diameters of electrospun nanofiber yarns as a function of electrospinning time. 50 measurements (five nanofiber yarns and ten diameter measurements along each yarn length) were used for determining average diameters. The uncertainty bars indicate one standard deviation.
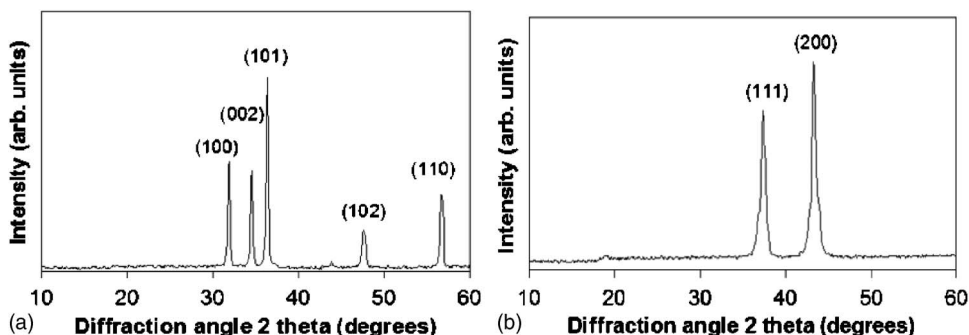
FIG. 4. XRD patterns of (a) zinc oxide and (b) nickel oxide nanofiber yarns (annealed at 873 K).

stant rate of fiber production and constant yarn density the slope of the diameter versus time curve should decrease with time as it takes increasing greater quantities of nanofiber for each incremental increase in yarn diameter. This suggests that the packing concentration of the nanofibers may decrease as the yarn diameter increases. This has not yet been verified experimentally.

2. X-ray diffraction

X-ray powder diffraction patterns were obtained with a Philips diffractometer employing Cu $K\alpha$ radiation, with 2θ in the range of 10°–60°, to examine the crystallinity of the zinc oxide and nickel oxide nanofiber yarns. The x-ray source was operated at 40 kV and 35 mA. The diffraction profiles of zinc oxide and nickel oxide nanofiber yarns annealed at 873 K are presented in Figs. 4(a) and 4(b). The x-ray diffraction (XRD) profiles indicated that both of the nanofiber structures are well crystallized after annealing at 873 K. The diffraction peaks for the zinc-based materials in Fig. 4(a) were identified to originate from the hexagonal zinc oxide crystal structure (Ref. 11; a=3.249 Å and c=5.205 Å). For the XRD pattern of the nickel oxide nanofibers, the (111) and (200) features of Fig. 4(b) can be indexed to the cubic nickel oxide phase with the lattice parameter a=4.174 Å.[12]

3. X-ray photoelectron spectroscopy

X-ray photoelectron spectroscopy (XPS) measurements were performed in a VG ESCALAB Mk II system under high vacuum conditions. The aluminum anode on a Mg/Al x-ray source was used at a power of 180 W with a fixed analyzer transmission energy of 50 eV. The major elements detected were Zn, Ni, and O, with a minor C feature, most likely due to adventitious carbon and organic residues, as shown in Figs. 5(a) and 5(b). No other impurities were detectable by XPS, thereby verifying the degradation and removal of the polymer precursors by annealing to 873 K. In particular, the nitrogen (N(1s)) feature near 400 eV which would result from PVP remnants is absent in Fig. 5. Low impurity levels will be important if electrospun nanofibers are to be used for photonics or sensor-related applications.

4. Auger electron spectroscopy (AES) imaging

In order to verify our XPS results and extend our surface characterization to the yarns, we also investigated nanofiber yarns by AES in the same ESCALAB chamber. In the case shown here, we also demonstrate one potential use of these nanofiber yarns which is to form twisted pairs of semiconducting metal oxide materials. Figure 6(a) shows a secondary electron image of a twisted pair of zinc oxide/nickel oxide nanofiber yarns, accompanied in Figs. 6(b) and 6(c) by coincident Auger images of Zn (in white) and Ni (in black). Figure 6(d) shows spectra formed by summing over each region, which clearly show the metals, carbon, and oxygen, but no nitrogen remnants from the PVP.

5. Ultraviolet-visible (UV-vis) spectroscopy

A U-3010 spectrophotometer was used to measure the absorption edge of the nanofiber yarns. The sample was prepared for spectroscopy measurement by grinding the nanofiber yarns to a fine powder. The optical absorbance of the samples was measured in the wavelength range of 200–800 nm. All sample spectra were acquired with respect to a powdered calcium fluoride (CaF_2) background. A semiconducting material exhibits minimal optical absorption for photons with energies smaller than the band gap and high absorption for photons with energies greater than the band gap. As a result, there is a sharp increase in absorption at energies close to the band gap that manifests itself as an
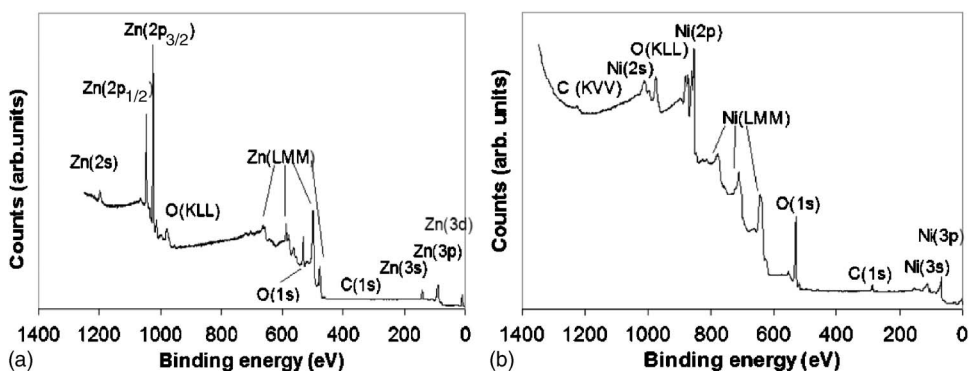

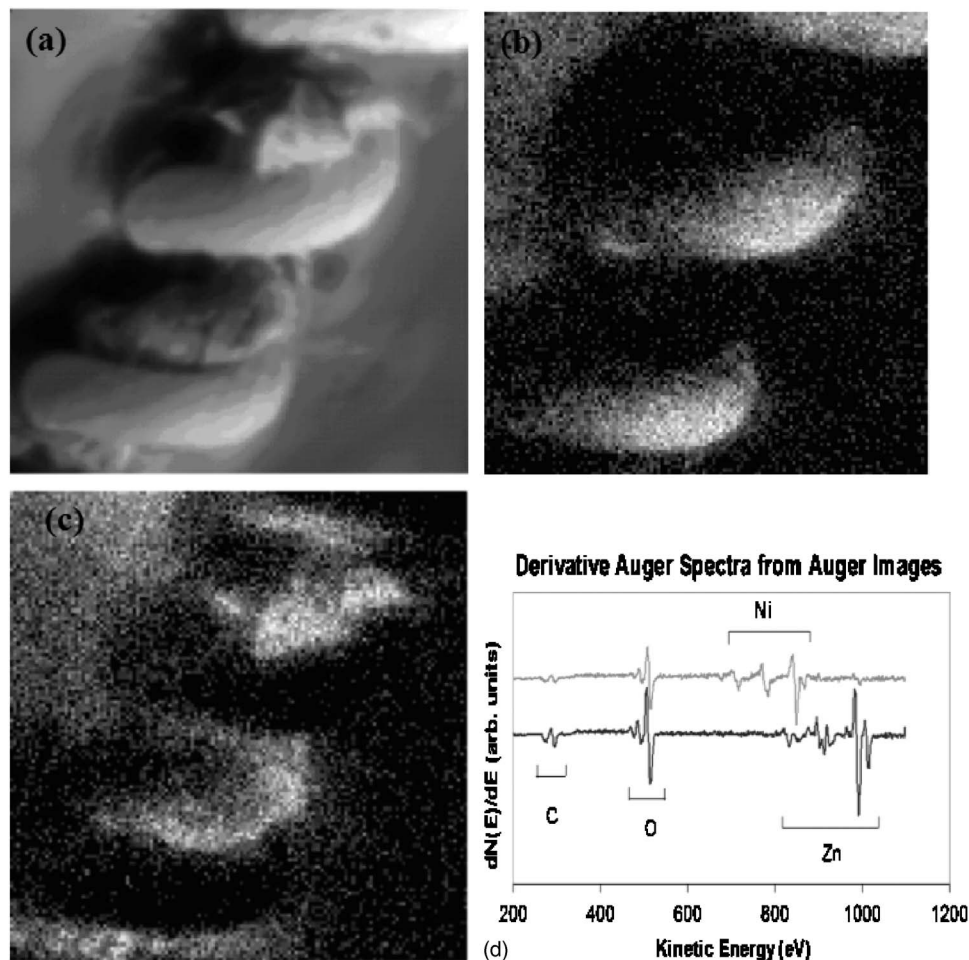FIG. 5. XPS spectra of (a) zinc oxide and (b) nickel oxide nanofiber yarns (annealed at 873 K).

FIG. 6. (a) Secondary electron image of twisted pair of zinc oxide/nickel oxide nanofiber yarn, (b) and (c) Auger electron images of Zn (white) and Ni (black), and (d) corresponding Auger electron spectra summed over each region of zinc oxide/nickel oxide nanofiber yarns.

absorption edge (or reflection threshold) in the UV-vis absorbance spectrum. UV-vis diffuse reflectance spectra of the metal oxide nanofibers calcined at 873 K are shown in Fig. 7. Based on these reflectance spectra the absorption edge for zinc oxide was found to be $\sim$26 000 cm^{-1} and that of nickel oxide was found to be $\sim$29 000 cm^{-1}. Using these absorption edge values, the band gap energies were calculated as 3.23 and 3.60 eV for zinc oxide and nickel oxide nanofibers, respectively, from the relationship of photon energy and freque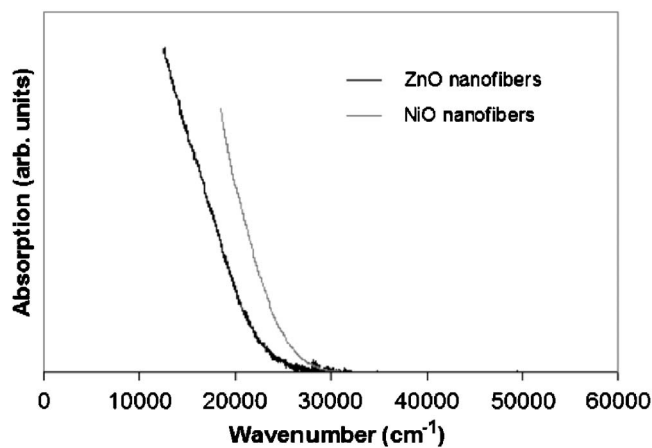ncy $E=h\nu$, where h is Planck's constant (6.626 $\times 10^{-34}$ J s) and $\nu=c/\lambda$; where c is the speed of light $(2.998\times10^8$ m/s) and λ is the wavelength of light. These absorption edges and calculated band gap energies are consistent with data reported in the literature for zinc oxide and nickel oxide materials.[13,14]

B. Electrical property characterization

1. Current-voltage (I-V) and conductivity measurements

In order to investigate the electrical properties of the metal oxide nanofiber yarns, *I-V* measurements were performed using a Keithley 2410 sourcemeter. In these experiments, a nanofiber yarn was placed on an insulating glass slide and contacts were made with silver paste to the ends of the yarn. Cu wires were connected to these contacts and voltages up to $\pm$50 V were applied. The room-temperature resistances of zinc oxide and nickel oxide nanofibers were 7.7×10^8 and 1.2×10^8 Ω, respectively, which are values consistent with those reported in the literature.[15]

The conductivities (σ, S/cm) of the metal oxide yarns as a function of temperature were calculated using their resistance R, length L, and cross sectional area A as $\sigma=L/RA$. For these experiments, an insulating glass substrate along with a nanofiber yarn attached was placed on a heating plate and covered with a porcelain lid to minimize convective losses. A thermocouple was placed in contact with the glass substrate to continuously monitor the temperature. Figure 8

FIG. 7. UV-vis spectra of zinc oxide and nickel oxide nanofibers (annealed at 873 K).
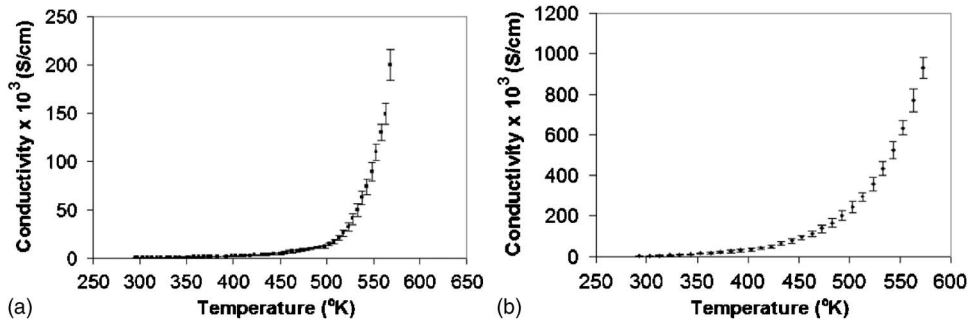
FIG. 8. Variation of electrical conductivities with temperature for (a) zinc oxide and (b) nickel oxide nanofiber yarns (annealed at 873 K).

shows how the conductivity changes from room temperature to 573 K. The voltage was kept constant at 35 V while the temperature was varied. The power dissipations due to current flow through the yarns were very small. Power dissipations of 0.35 and 2.68 mW were found for zinc oxide and nickel oxide yarns, respectively, at temperature of 573 K. The conductivity increased with increasing temperature for both zinc oxide and nickel oxide nanofiber yarns, suggesting semiconducting behavior is expected for these materials.[16]

2. Activation energy determination

Figures 9(a) and 9(b) show plots of the natural log of conductivity versus inverse temperature (ln σ versus $1/T$) for the zinc oxide and nickel oxide nanofiber yarns annealed at 873 K, respectively. Thermal activation energies were extracted from the slopes. The activation energy connects the conductivity to the temperature in an Arrhenius-type relationship,

$$\sigma = \sigma_0 \exp\left(\frac{-E_a}{k_B T}\right), \qquad (1)$$

where σ_0 is the preexponential factor, E_a is the activation energy, k_B is Boltzmann's constant, and T is the absolute temperature. Because most zinc oxide materials are strongly *n*-type, it has long been assumed that the dominant donor is a native defect, either an oxygen vacancy or an interstitial Zn site.[17,18] Similarly, undoped nickel oxide is a defect semiconductor in which the resistivity strongly depends on the concentration of cation (Ni) vacancies.[19]

The best linear fits to the data of Fig. 9 require the selection of different temperature regions, i.e., regions I–III for the zinc oxide nanofiber yarn and two different regions for nickel oxide nanofiber yarn. The corresponding values of thermal activation energies are tabulated in Table I. The different regions in the ln σ versus $1/T$ curves for zinc oxide

and nickel oxide arise from different conduction processes in the corresponding semiconducting nanofibers. This could be attributed to the appearance of trap states due to chemisorption of oxygen and water vapor at the grain boundaries. For example, in our nickel oxide nanofiber yarns, two activation energies were found below the conduction bands at 0.20 and 0.40 eV, which are close to a reported value of 0.39 eV for the temperature range of 373–573 K.[20]

It should be noted that the conductivity of our zinc oxide nanofibers was found to increase after aging in ambient atmosphere, while that of nickel oxide decreased. The trends of these conductivity changes are consistent with the reported literature for such materials.[21,22] For zinc oxide the change can be attributed to oxide surface modification with the formation of a conducting deposit in the presence of humidity and reducing gases (e.g., carbon monoxide) in air. Yarns of nanofibers having high surface area to volume ratio should be especially susceptible to the effects of atmospheric gases. For example, carbon monoxide reacts with chemisorbed oxygen on zinc oxide surface layers, allowing electrons to be donated to the conduction band. This process increases the electron density, and hence the conductivity of zinc oxide.[21] In the case of nickel oxide, it is possible that residual stress and microstructural defect recovery may be the reason for the observed variations in conductivity with time of our nanofibers.[22]

IV. CONCLUSIONS

Twisted yarns of metal oxide nanofibers were made using an electrospinning apparatus having a rotating collector and a stationary collector. The yarn structure enabled easy handling and electrical property measurements. Conductivity changes with temperature show that undoped zinc oxide and nickel oxide nanofiber yarns behave similar to their sol-gel thin film counterparts. These zinc oxide and nickel oxide
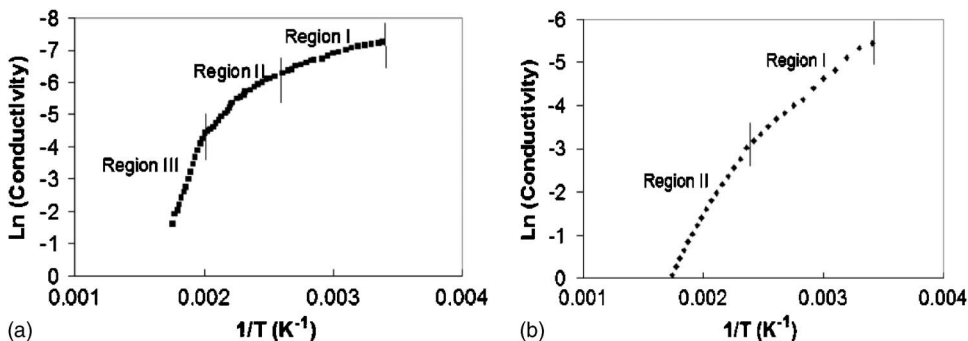

FIG. 9. Arrhenius plots for (a) zinc oxide and (b) nickel oxide nanofiber yarns (annealed at 873 K).

TABLE I. Thermal activation energies of zinc oxide and nickel oxide nanofibers in different temperature ranges.

Sample	Temperature range (K)	Activation energy (eV)
ZnO nanofiber yarn	293–423	0.10 ± 0.01
	423–513	0.26 ± 0.01
	513–573	1.03 ± 0.08
NiO nanofiber yarn	293–423	0.20 ± 0.01
	423–573	0.40 ± 0.03

nanofibers and their corresponding yarns have potential for applications in catalytic, photocatalytic, electronic, and sensor devices.

ACKNOWLEDGMENTS

[1] J. Doshi and D. H. Reneker, J. Electrost. **35**, 151 (1995).
[2] D. H. Reneker, A. L. Yarin, H. Fong, and S. Koombhongse, J. Appl. Phys. **87**, 4531 (2000).
[3] A. Theron, E. Zussman, and A. L. Yarin, Nanotechnology **12**, 384 (2001).
[4] K. H. Lee, Y. H. Kim, M. S. Khil, Y. M. La, and D. R. Lee, Polymer **44**, 1287 (2003).
[5] A. L. Yarin, S. Koombhongse, and D. H. Reneker, J. Appl. Phys. **89**, 3018 (2000).
[6] C. E. Schmidt and J. B. Leach, Annu. Rev. Biomed. Eng. **5**, 293 (2003).
[7] W. E. Teo and S. Ramakrishna, Nanotechnology **16**, 1882 (2005).
[8] S. F. Fennessey and R. J. Farris, Polymer **45**, 4217 (2004).
[9] P. D. Dalton, D. Klee, and M. Moller, Polymer **46**, 611 (2005).
[10] S. Doiphode and D. H. Reneker, Book of Abstracts, The Americal Physical Society, Spring meeting, March, 2006 (unpublished).
[11] JCPDS Card No. 36-1451.
[12] JCPDS Card No. 47-1049.
[13] M. Ohyama, H. Kozuka, and T. Yoko, Thin Solid Films **306**, 83 (1997).
[14] A. B. Kunz, J. Phys. C **14**, L445 (1981).
[15] B. Ismail, M. Abaab, and B. Rezig, Thin Solid Films **383**, 93 (2001).
[16] Z.-P. Sun, L. Liu, L. Zhang, and D. Z. Jia, Nanotechnology **17**, 2268 (2006).
[17] G. Heiland, E. Mollwo, and F. Stöckmann, in *Solid State Physics*, edited by F. Seitz and D. Turnbull (Academic, New York, 1959), Vol. 8, p. 191.
[18] F. A. Kröger, *The Chemistry of Imperfect Crystals* (North-Holland, Amsterdam, 1974).
[19] M. A. Wittenhauer and L. L. Van Zandt, Philos. Mag. B **46**, 659 (1982).
[20] S. Song and P. Xiao, Mater. Sci. Eng., A **A323**, 29 (2002).
[21] B.-k. Na, M. A. Vannice, and A. B. Walters, Phys. Rev. B **46**, 12266 (1992).
[22] H. L. Chen, Y. M. Lu, and W. S. Hwang, Surf. Coat. Technol. **198**, 141 (2005).